

# Geometric Frustration in Buckled Colloidal Monolayers

Y. Han,<sup>1,2,\*</sup> Y. Shokef,<sup>1,\*</sup> A. M. Alsayed,<sup>1</sup> P. Yunker,<sup>1</sup> T. C. Lubensky,<sup>1</sup> and A. G. Yodanis<sup>1</sup>

<sup>1</sup>Department of Physics and Astronomy, University of Pennsylvania, Philadelphia, PA 19104, USA

<sup>2</sup>Department of Physics, Hong Kong University of Science and Technology, Clear Water Bay, Kowloon, Hong Kong

(Dated: November 2, 2018)

Geometric frustration arises when lattice structure prevents simultaneous minimization of local interactions. It leads to highly degenerate ground states and, subsequently, complex phases of matter such as water ice, spin ice and frustrated magnetic materials. Here we report a simple geometrically frustrated system composed of closely packed colloidal spheres confined between parallel walls. Diameter-tunable microgel spheres are self-assembled into a buckled triangular lattice with either up or down displacements analogous to an antiferromagnetic Ising model on a triangular lattice. Experiment and theory reveal single-particle dynamics governed by in-plane lattice distortions that partially relieve frustration and produce ground-states with zigzagging stripes and subextensive entropy, rather than the more random configurations and extensive entropy of the antiferromagnetic Ising model. This tunable soft matter system provides an uncharted arena in which the dynamics of frustration, thermal excitations and defects can be directly visualized.

Geometric frustration arises in physical and biological systems<sup>1</sup> ranging from water<sup>2</sup> and spin ice<sup>3</sup> to magnets<sup>4,5</sup>, ceramics<sup>6</sup>, and high- $T_c$  superconductors<sup>7</sup>. The essence of this phenomenon is best captured in the model of Ising spins arranged on a two-dimensional (2D) triangular lattice and interacting anti-ferromagnetically<sup>8,9</sup>; two of the three spins on any triangular plaquette within this lattice can be antiparallel to minimize their anti-ferromagnetic (AF) interaction energy, but the third spin is *frustrated* because it cannot be simultaneously antiparallel to both neighbouring spins (Fig. 1A). Such frustration leads to materials with many degenerate ground states and extensive entropy proportional to the number of particles in the system. Consequently, small perturbations can introduce giant fluctuations with peculiar dynamics. Traditionally, these phenomena have been explored in atomic materials by ensemble averaging techniques such as neutron and X-ray scattering, muon spin rotation, nuclear magnetic resonance, and heat capacity and susceptibility measurements<sup>5</sup>. More recently, artificial arrays of mesoscopic constituents have been fabricated in order to probe geometric frustration at the single-‘particle’ level. Examples of the latter include Josephson junctions<sup>10</sup>, superconducting rings<sup>11</sup>, ferromagnetic islands<sup>12,13,14</sup>, and recent simulations<sup>15</sup> of charged colloids in optical traps. Observations in these model systems, however, have been limited to the static patterns into which these systems freeze when cooled. Thus many questions about frustrated systems remain unexplored, particularly

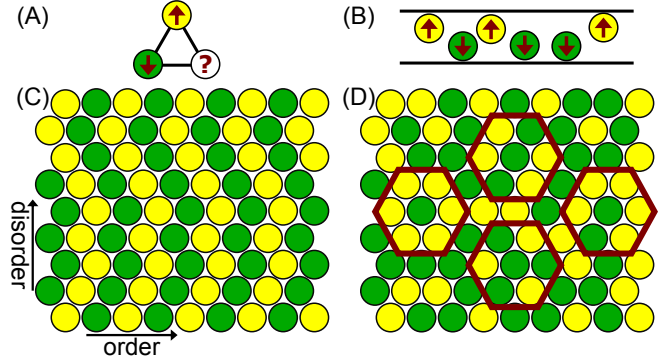


FIG. 1: **Ising ground state.** (A) Three spins on a triangular plaquette cannot simultaneously satisfy all AF interactions. (B) For colloids confined between walls separated of order 1.5 sphere diameters (side view), particles move to opposite walls in order to maximize free volume. (C,D) Ising ground state configurations wherein each triangular plaquette has two satisfied bonds and one frustrated bond. (C) Zigzag stripes generated by stacking rows of alternating up/down particles with random sideways shifts; all particles have exactly 2 frustrated neighbours. (D) Particles in disordered configurations have 0, 1, 2, or 3 frustrated neighbours (red hexagons).

those associated with single-particle dynamics. For example, how, when, and why do individual particles change states to accommodate their local environments, and what kinetic mechanisms govern transitions to glassy phases?

Here we report on the static and *dynamic* properties of a self-assembled colloidal system analogous to Wannier’s AF Ising model<sup>8</sup>. Densely packed spheres between parallel walls form an in-plane triangular lattice with out-of-plane up and down buckling<sup>16,17,18,19,20,21,22,23,24,25,26</sup>. The up-down states of the spheres produced by buckling are analogous to up-down states of Ising spins (Fig. 1B). Nearest-neighbour excluded volume interactions between particles favour opposite states for neighbouring particles, as do the AF interactions between neighbouring spins in the Ising model. In contrast to engineered mesoscopic systems<sup>10,11,12,13,14</sup>, however, the colloidal system facilitates easy *tuning* of the effective AF interaction through changes in the diameter of temperature-sensitive microgel spheres<sup>27</sup>. The colloidal system also permits direct visualization of thermal motion at the *single-particle* level. In the limit of weak confinement, or weak interaction strength, system properties closely follow those predicted for the AF Ising model, but in the limit of strong confinement, they do not. For strong interactions, the lattice deforms to maximize free volume, and the collective nature of the free-volume-dominated free energy characteristic of most soft-matter systems becomes important. We understand these effects the-

\*These authors contributed equally to this work.

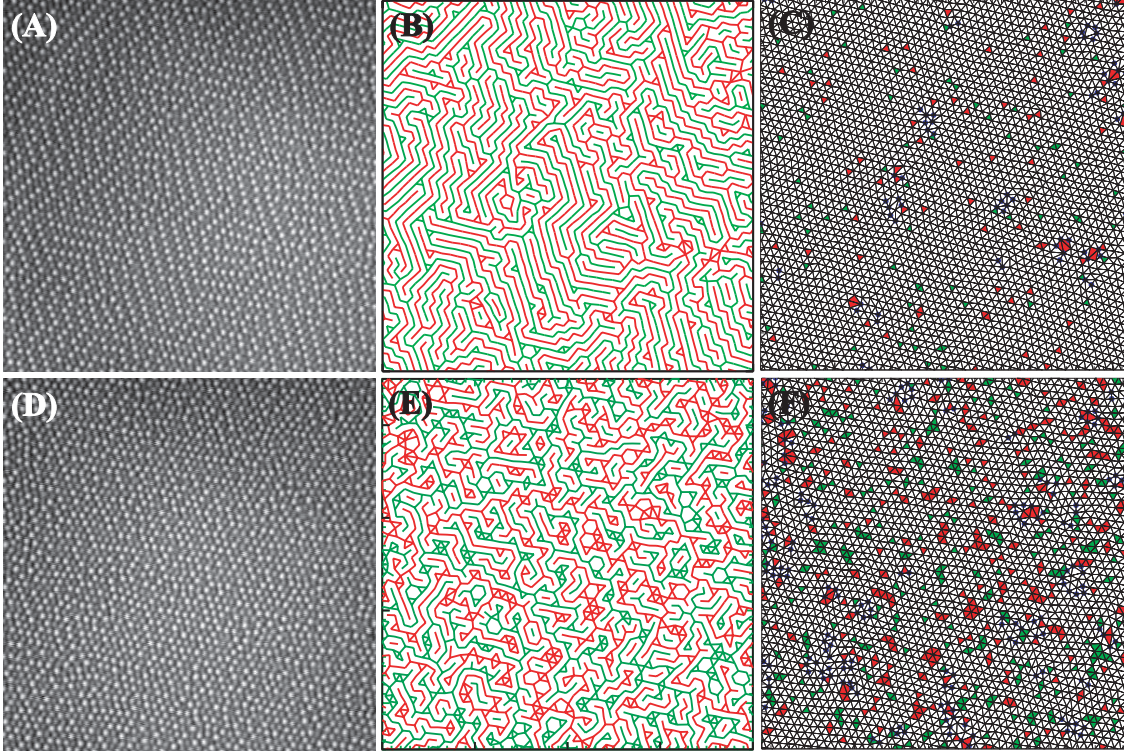


FIG. 2: **Buckled monolayer of colloidal spheres.** Movies are in **Supplementary Information**.  $(32\ \mu\text{m})^2$  area at  $T = 24.7^\circ\text{C}$  (A-C) and  $27.1^\circ\text{C}$  (D-F). (A, D): Bright spheres: up; dark spheres: down. (B, E): Labyrinth patterns obtained by drawing only the frustrated up-up (red) and down-down (green) bonds. (C, F): Corresponding Delaunay triangulations. Blue dots mark defects in the triangular lattice, i.e. particles that do not have exactly six nearest neighbours. Thermally excited triangles with three spheres up/down are labelled by red/green.

oretically in terms of tiling of the plane by isosceles triangles. The tiling scheme identifies a ground-state consisting of zigzagging stripes with sub-extensive entropy. Interestingly, in contrast to Ising-model predictions, first measurements of single-particle ‘spin-flipping’ suggest that flipping dynamics depend not only on the number of nearest-neighbour frustrated ‘bonds’, but on how these bonds are arranged. Thus the paper begins to explore connections between frustrated soft matter and hard materials such as frustrated AF media.

**Experimental System.** For walls separated by distances on order 1.5 sphere diameters, the particles maintain in-plane triangular order (see Supplementary Information) but buckle out-of-plane (Fig. 2, A, D). This buckling minimizes system free energy,  $F = U - TS$ , where  $U$  is the internal energy,  $T$  temperature, and  $S$  entropy; spheres move apart to lower their repulsive interaction potential energy  $U$  and to increase their free volume  $V$ , which in turn leads to an entropy increase with  $S \propto \ln V$ . The effective repulsion causes spheres to move to the top or bottom wall, and nearest-neighbours maximize free volume by moving to opposite walls (Fig. 1B). Buckled colloidal monolayers were first observed more than two decades ago<sup>16,17,18</sup>, and the AF analogy was then suggested<sup>17,28</sup>. However, to date, few quantitative measurements have been performed on this system class, and the themes explored by most of the early work centred largely on structural transitions exhibited by colloidal thin films as a function of increasing sample thickness<sup>17,18,19,20,22,23,24</sup>, rather than their connection to frustrated anti-ferromagnets. The use

of temperature-sensitive *diameter-tunable* NIPA (N-isopropyl acrylamide) microgel spheres<sup>27</sup> also distinguishes our experiments from earlier work. By varying temperature we change particle size and sample volume fraction and, therefore, vary the strength of the effective AF interparticle interactions.

Samples were annealed at low volume fraction near the melting point to produce 2D crystal domains with  $\sim 10^5$  spheres covering an area of order  $(60\ \mu\text{m})^2$ . Video microscopy measurements were carried out far from grain boundaries on a  $\sim (32\ \mu\text{m})^2$  central area ( $\sim 2600$  spheres) within the larger crystal domain. Particle motions were observed by microscope, recorded to videotape using a CCD camera and tracked by standard image-processing techniques<sup>29</sup>. Our colloids are very weakly charged<sup>27</sup> and were measured to have *short-ranged* repulsive interactions<sup>30</sup>. Furthermore, NIPA spheres are nearly density matched in water, so gravitational effects are negligible. In most colloid experiments the important thermodynamic control variable is particle volume fraction. The present experiment achieved substantial variation in sphere diameter using small changes in temperature, which altered thermal energies by less than 1%. In this paper we monitor and report temperature rather than volume fraction because the interactions between spheres contain a soft tail that introduces some ambiguity into the assignment of a geometric diameter to the particles. Below  $24^\circ\text{C}$  the system is jammed and no dynamics are observed. Above  $27.5^\circ\text{C}$  the in-plane crystals melt. Our primary measurements of the frustrated states probe five temperatures from  $24.7^\circ\text{C}$  to  $27.1^\circ\text{C}$  in  $0.6^\circ\text{C}$  steps.



In this range, the hydrodynamic diameter of the particles decreases linearly with increasing temperature from  $0.89 \mu\text{m}$  to  $0.76 \mu\text{m}$ , while the average in-plane particle separation remains  $0.7 \mu\text{m}$ . To reach thermal equilibration, the sample was annealed near the melting point before the temperature was slowly decreased. No hysteresis was observed when slowly cycling through this temperature range.

**Anti-Ferromagnetic Order.** The images in Fig. 2, A, D show roughly half of the spheres as bright because they are in the focal plane of the microscope; the other half, located near the bottom plate, are slightly out-of-focus and appear dark. We discretize the continuous brightness profile of the particles into two ‘Ising’ states with  $s_i = \pm 1$ . The nature of the frustrated states can be exhibited in different ways in processed images. One way focuses on the ‘bonds’ between particles. We refer to pairs of neighbouring particles in opposite states ( $s_i s_j = -1$ ) as satisfied bonds, i.e. satisfying the effective AF interaction, and to up-up or down-down pairs (with  $s_i s_j = 1$ ) as frustrated bonds. Images of these bonds show that the frustrated bonds form a nearly single-line labyrinth (Fig. 2B) at low temperature that then nucleates into domains (Fig. 2E) at high temperature. Local AF order is alternatively characterized by the average number of frustrated bonds per particle,  $\langle N_f \rangle$ . In the limit of weak interactions, an Ising system chooses a completely random configuration with half of the six bonds satisfied and half frustrated, leading to  $\langle N_f \rangle = 3$ . In the limit of strong interactions, on the other hand, each triangular plaquette has one frustrated bond (Fig. 1A), a third of the bonds are frustrated, and  $\langle N_f \rangle = 2$ .  $\langle N_f \rangle$  is a linear rescaling of the density of excited triangles (3 up or 3 down) in Fig. 2, C, F, which ranges from 0 in the Ising ground state to 0.5 for a random configuration. We find that  $\langle N_f \rangle$  decreased from approximately 2.5 to 2.1 in the temperature interval  $27.1^\circ\text{C}$ – $24.7^\circ\text{C}$ . Detailed statistics of the different local configurations are presented in Supplementary Table S1.

We first consider the static properties of the frustrated samples. In particular we aim to identify similarities and differences between the colloidal system and the Ising model. As the temperature is lowered to increase the particle diameter,  $\langle N_f \rangle$  is observed to approach 2. This behaviour is expected in the Ising model ground state. However, the vast majority of Ising ground-state configurations are disordered. The colloidal monolayers, by contrast, condense into stripe phases. The stripes are not straight, as could be produced by higher-order interparticle interactions<sup>31</sup>. Rather they bend and form zigzag patterns<sup>22,23,24,25,26</sup> (see Fig. 2A and Supplementary Table S1). In this colloidal zigzag striped phase, we measured spatial correlations  $\Gamma(i-j) = [\langle s_i s_j \rangle - \langle s \rangle^2] / [\langle s^2 \rangle - \langle s \rangle^2]$  over separations  $|i-j|$ , along the principal lattice directions, of up to 20 particles and found that they decay exponentially in magnitude with alternating sign (Supplementary Fig.S4).  $\Gamma(i-j)$  is positive for  $i-j$  even and negative for  $i-j$  odd. In contrast,  $\Gamma(i-j)$  averaged over the Ising ground state is positive when  $i-j$  is an integer multiple of 3. Furthermore, for zigzagging stripes each particle has exactly two frustrated neighbours (Fig. 1C), whereas in the fully disordered Ising ground-state  $N_f$  can be 0, 1, 2, or 3 (Fig. 1D) and only the average  $\langle N_f \rangle$  is 2. These observations suggest that fluctua-

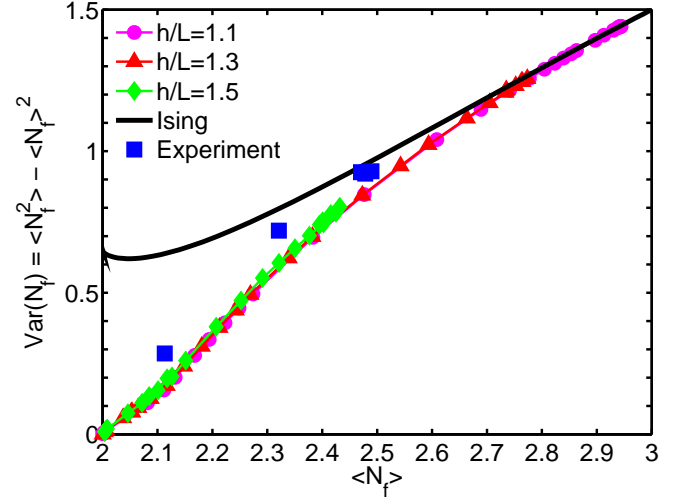


FIG. 3: **Fluctuation in the number of frustrated bonds per particle as a function of its average.** Experiments quantitatively agree with hard-sphere simulations at different plate separations  $h$ , normalized by the average in-plane lattice constant  $L$ . Simulations collapse onto a single curve and deviate significantly from the behaviour in the Ising model.

tions in  $N_f$ , i.e.  $\text{Var}(N_f) = \langle N_f^2 \rangle - \langle N_f \rangle^2$ , might be a useful measure for distinguishing the zigzag stripe phase observed here from the disordered Ising ground-state. Figure 3 plots the behaviour of  $\text{Var}(N_f)$  as a function of  $\langle N_f \rangle$  for the Ising model and for data obtained both from experiments and from hard-sphere Monte Carlo (MC) simulations. Results from experiment and simulation agree at both low and high volume fraction and differ from those of the Ising model, especially at high volume fraction wherein interactions are strong.

**Zigzagging Stripes.** Ideal geometrically frustrated systems, such as the AF Ising model, are highly degenerate with extensive entropy at zero temperature. However, in real materials, subtle effects, for example anisotropic interactions<sup>9</sup>, long-range interactions<sup>31</sup>, boundary conditions<sup>32</sup> and lattice distortions<sup>33,34</sup> relieve frustration. Our partially ordered zigzag stripe phase at high volume fraction is an example of frustration relief by lattice distortion. In the colloidal monolayer the triangular packing is self-assembled, and (like atoms in real solids) the particles are not forced to remain at fixed positions on the lattice<sup>26</sup>. This deformability and the fact that the free volume of the system is a collective function of all particle positions breaks the mapping to simple Ising models with pair-wise additive nearest neighbour interactions. In fact, the positions of the colloidal particles may be thought of as comprising a planar structure that crumples between the two confining planes. This ‘‘crumpling’’ leads to deformations of the planar triangular lattice with satisfied bonds (projected onto the plane) on average 3 – 4% shorter than frustrated bonds. This difference is consistent with the notion that each pair of neighbouring particles prefers to be separated by the *same fixed distance* in 3D, whether or not their connecting bond is satisfied.

A simple tiling argument demonstrates why the colloidal

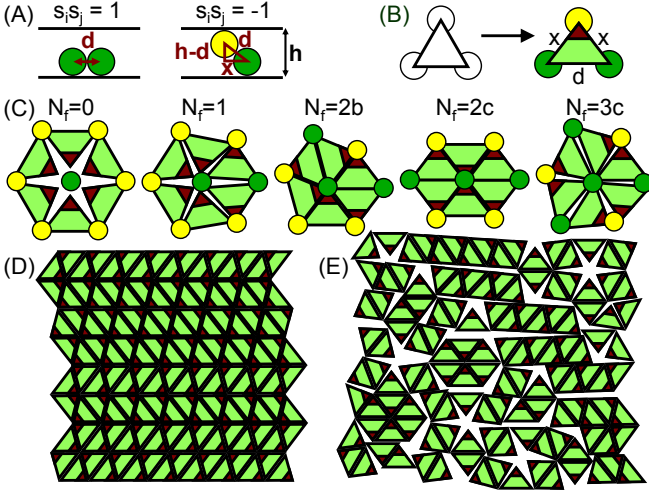


FIG. 4: **Tiling the plane with isosceles triangles.** (A) Close-packed spheres are separated by one particle diameter  $d$  in 3D. This distance projected on the 2D plane remains  $d$  for a frustrated bond ( $s_i s_j = 1$ ), but is reduced to  $x = \sqrt{d^2 - (h - d)^2}$  for a satisfied bond ( $s_i s_j = -1$ ). (B) Viewed from above, each plaquette in the lattice tends to deform to an isosceles triangle with one long side ( $d$ ) along the frustrated bond and two short sides ( $x < d$ ) along the satisfied bonds. The angle larger than  $\pi/3$  is marked in red. (C) All possible in-plane local particle configurations appearing in the Ising ground state. The isosceles triangles can tile the plane without extra space only for  $N_f = 2$ . The “white space” for  $N_f = 0, 1, 3$  corresponds to additional excluded volume. (D, E) Tilings corresponding to striped and disordered Ising ground-state configurations, respectively, of Fig. 1, C, D.

system ground-state configurations of stripes and zigzag pack better than the disordered Ising configurations. Furthermore, the tiling model shows explicitly that maximal volume fractions of stripe and zigzag phases are the same. Each triangular plaquette in the Ising ground-state contains two satisfied bonds and one frustrated bond. Thus, when spheres are close-packed in 3D, the equilateral triangle defined by each such triplet of neighbouring particles is tilted, and when projected onto the 2D plane, it deforms into an isosceles triangle with two short sides along the satisfied bonds and one long side along the frustrated bond (Fig. 4, A, B). Subsequently, close-packed configurations of the buckled spheres in 3D are described by tilings of the plane by isosceles triangles. Figure 4C shows the configurations of isosceles triangles for different numbers of frustrated bonds ( $N_f$ ) in the basic hexagonal cell. By summing up the angles around the central vertex, one immediately sees that for  $N_f = 0, 1, 3$ , the triangles cannot close-pack. Only the two configurations with  $N_f = 2$  enable tiling the plane with isosceles triangles, or, equivalently, close-packing of the buckled spheres in 3D. Configuration 2b corresponds to a bend in a stripe, and 2c to a stripe continuing along a straight line. Both have the same maximal volume fraction, thus corroborating observations of zigzagging stripes in the experiments and simulations.

Experiments and simulations indicate a preference of the stripes to form straight segments rather than to bend eas-

ily and thus to generate randomly zigzagging configurations (Fig. 2A). Zigzagging stripes can be viewed as a random stack of ordered lines of alternating up and down particles (Fig. 1C), thus straight and zigzagging stripes are analogous to the face-centred cubic (FCC) lattice and the random hexagonal-close-packed (RHCP) structure<sup>20</sup> in 3D. Straight and zigzagging stripes are equivalent in the close-packed limit by having the same maximal volume fraction. However, for smaller volume fractions there may be an order-by-disorder effect<sup>5,35</sup>, giving a small free volume advantage of straight stripes over zigzagging ones, similar to the free volume advantage<sup>36</sup> of FCC over RHCP in 3D.

Instead of an extensive entropy at zero temperature<sup>8</sup>, wherein  $S$  scales linearly with the number  $N$  of particles in the system, here the entropy is subextensive. The number of zigzagging striped configurations grows exponentially with the linear dimension of the system (there are two possible ways of placing one row relative to its predecessor in Fig. 1C), hence the entropy scales<sup>37</sup> as  $\sqrt{N}$ . Alternatively put, a non-branching single-line labyrinth is dictated by the particles on the boundary, and for the system to rearrange from one zigzag stripe configuration to another, a percolating cluster of order  $\sqrt{N}$  particles should be flipped.

**Dynamics.** Taken together these observations have interesting consequences for the ground-state dynamics of frustrated systems. The Ising ground-state has a local zero-energy mode, as shown in configuration 3c in Fig. 5A: the central particle can flip without changing the energy of the system, thus rapidly relaxing spin correlations via a sequence of such single spin flips, even at zero temperature. For buckled spheres, on the other hand, the close-packed configurations have only particles with  $N_f = 2$ , and, moreover, even a particle with  $N_f = 3$  in an excited configuration has to cross an energy barrier in order to flip. Like the glassy behavior of an Ising model on a deformable lattice<sup>38,39</sup>, the slow dynamics we observe at low temperature is a consequence of the absence of local zero-energy modes in the bulk. Subextensive ground-state entropy also appears in related models emulating systems with glassy dynamics<sup>40</sup>.

Online movies (see Supplementary Information) permit us to directly visualize ‘spin flipping’ as well as the motions of thermal excitations and defects in frustrated systems for the first time. Thermal excitations labelled as coloured triangles in Fig. 2, C, F were typically found to be generated/annihilated in pairs due to the flipping of a particle shared by the two triangles. Well-isolated thermal excitations, on the other hand, appear to be more stable. To quantify these effects, we first extract the full time trajectory,  $s_i(t)$ , of each particle  $i$  from the movies. In Fig. 5B we plot the single particle autocorrelation function  $C(t) = [\langle s_i(t)s_i(0) \rangle - \langle s_i \rangle^2] / [\langle s_i^2 \rangle - \langle s_i \rangle^2]$ , averaged over all particles not at lattice defects. As the temperature is lowered, the correlation function develops a stretched exponential form,  $C(t) = \exp[-(t/\tau)^\beta]$ . The measured relaxation time  $\tau$  exhibits a dramatic increase as the particles swell at low temperature, while the extracted stretching exponent  $\beta$  decreases, indicating slow dynamics similar to those found in glasses.

To further explore the dynamics of different local configu-

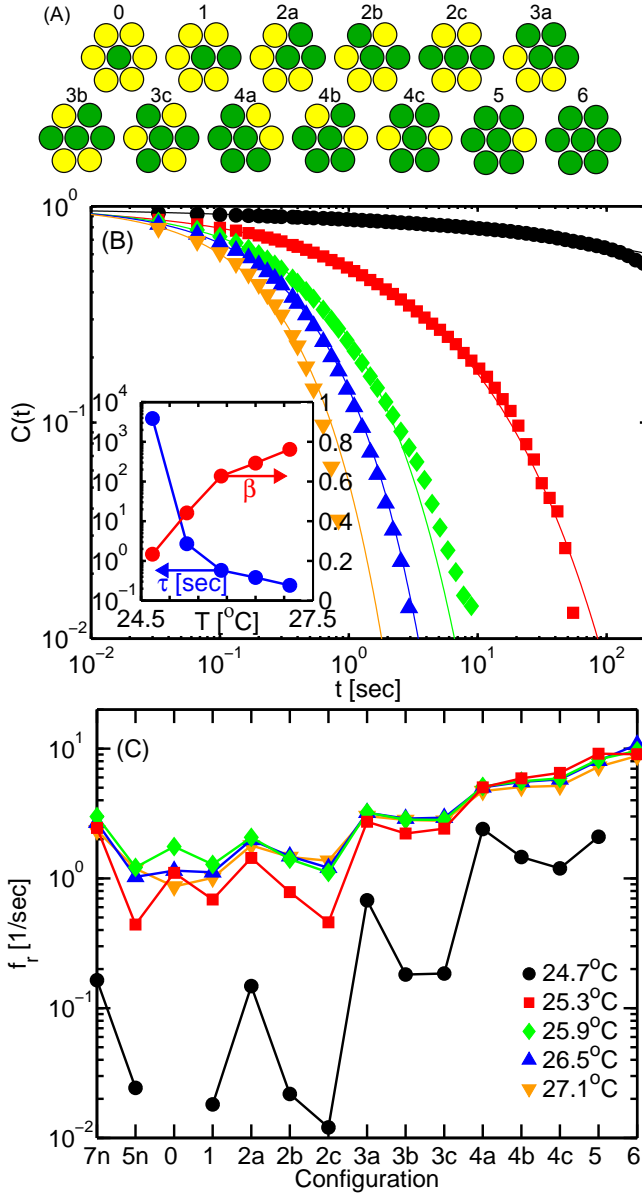


FIG. 5: **Single particle dynamics.** (A) Local configurations are labelled by their value of  $N_f$  and an index a,b,c indicating the precise geometrical arrangement of the frustrated neighbours for  $N_f = 2, 3, 4$ . Symmetry to rotation and inversion reduces the  $2^7$  possible configurations to the 13 given here. (B) Single particle autocorrelation functions plotted versus decay time. Lines are fits to stretched exponentials  $C(t) = \exp[-(t/\tau)^\beta]$ , with  $\tau$  and  $\beta$  given in the inset. (C) Flipping rates for the different local environments. Configurations 7n and 5n are defects in the in-plane lattice, with 7 and 5 nearest neighbours.

rations (defined in Fig. 5A), Fig. 5C shows the flipping rate  $f_r$  of single particles with a fixed neighbour structure. We measured the probability  $p$  that a particle flips between consecutive images given that the Ising states of its neighbours remained unchanged. The time intervals of  $dt = 1/30$  sec between frames were short enough such that  $p$  was typically

small (0.36 at most) and the flip rate could be approximated by  $f_r = p/dt$ . At high temperature, the behaviour is similar to that of an Ising model undergoing Glauber dynamics:  $f_r \sim e^{-\Delta E/k_B T}$  where the energy difference  $\Delta E$  is proportional to the difference in  $N_f$  before and after flipping. In this regime, particles with large  $N_f$  flip slightly more slowly at higher temperature because of the weaker interactions between spheres. As the volume fraction is increased by lowering the temperature, the particle dynamics slow by 1-2 orders of magnitude and, more interestingly, *significant differences develop between different geometrical configurations with the same  $N_f$* . Such phenomena may not appear in the simple Ising model where the Hamiltonian depends only on  $N_f$ .

Defects in the underlying lattice can strongly affect the properties of frustrated systems. However, detailed knowledge about the role of defects in frustrated systems is very limited. Our experiments permit us to directly visualize defects nucleating, annihilating, and diffusing (see Supplementary Information movies). By comparing trajectories containing different numbers and types of defects, our initial studies suggest that defect particles have enhanced in-plane diffusion (Supplementary Fig. S5) and slower flipping dynamics than averaging over particles with six nearest neighbours.

**Conclusion.** We have presented experimental measurements of single-particle dynamics in a geometrically frustrated system. Colloidal spheres with tunable diameter self-assemble to buckled monolayer crystals and form a system analogous to the triangular lattice AF Ising model. By tuning the volume fraction, we found that at high compaction, in-plane lattice deformation relieves most frustration and yields a zigzag stripe ground-state with subextensive entropy. The ‘free spins’ in the Ising ground state are removed; thus the system become glassy as the volume fraction is increased. A theoretical analysis shows that these features can be captured by a hard-sphere model. We measured spatial correlations and the statistics of various local configurations as well as their flipping rates and found strong dependences on arrangements of neighbouring particles. As the glassy phase is approached, we observed dramatic slowing of the dynamics and formation of stretched exponential correlation functions. Single-defect dynamics were directly visualized and measured for the first time. Defects have faster in-plane diffusion and slower out-of-plane flipping than the average.

Our demonstration and analysis of this self-organized colloidal ‘antiferromagnet’ opens the door for the study of detailed single-particle dynamics in frustrated systems and begins an exploration of the connections between frustrated soft materials and the more studied frustrated magnetic materials. Many further manipulations can be readily applied to this system, e.g. external control of particle motions with optical tweezers, gravitational fields, electric fields, different particle interactions, and defect doping. Theoretically, it will be interesting to consider possible modifications to the Ising model that generate a zigzagged stripe ground state and to study the glassy dynamics arising from its subextensive zero-temperature entropy.

1. Moessner, R. & Ramirez, A. R. Geometrical frustration. *Phys. Today* **59**, 24-26 (2006).
2. Pauling, L. The structure and entropy of ice and of other crystals with some randomness of atomic arrangement. *J. Am. Chem. Soc.* **57**, 2680-2684 (1935).
3. Harris, M. J., Bramwell, S. T., McMorrow, D. F., Zeiske, T. & Godfrey, K. W. Geometrical frustration in the ferromagnetic pyrochlore  $\text{Ho}_2\text{Ti}_2\text{O}_7$ . *Phys. Rev. Lett.* **79**, 2554-2557 (1997).
4. Bramwell, S. T. & Gingras, M. J. P. Spin ice state in frustrated magnetic pyrochlore materials. *Science*, **294**, 1495-1501 (2001).
5. Moessner, R. Magnets with strong geometric frustration. *Can. J. Phys.* **79**, 1283-1294 (2001).
6. Ramirez, A. R. Geometric frustration: Magic moments. *Nature* **421**, 483 (2003).
7. Anderson, P. W. The resonating valence bond state in  $\text{La}_2\text{CuO}_4$  and superconductivity. *Science*, **235**, 1196-1198 (1987).
8. Wannier, G. H. Antiferromagnetism. the triangular Ising net. *Phys. Rev.* **79**, 357-364 (1950); erratum *Phys. Rev. B* **7**, 5017 (1973).
9. Houtappel, R. M. F. Order-disorder in hexagonal lattices. *Physica* **16**, 425-455 (1950).
10. Davidović, D. *et al.* Correlations and disorder in arrays of magnetically coupled superconducting rings. *Phys. Rev. Lett.* **76**, 815-818 (1996).
11. Hilgenkamp, H. *et al.* Ordering and manipulation of the magnetic moments in large-scale superconducting  $\pi$ -loop arrays. *Nature* **422**, 50-53 (2003).
12. Wang, R. F. *et al.* Artificial 'spin ice' in a geometrically frustrated lattice of nanoscale ferromagnetic islands. *Nature* **439**, 303-306 (2006).
13. Möller, G. & Moessner, R. Artificial square ice and related dipolar nanoarrays. *Phys. Rev. Lett.* **96**, 237202 (2006).
14. Nisoli, C., *et al.* Ground state lost but degeneracy found: the effective thermodynamics of artificial spin ice. *Phys. Rev. Lett.* **98**, 217203 (2007).
15. Libál, A., Reichhardt, C. & Reichhardt, C.J.O. Realizing colloidal artificial ice on arrays of optical traps. *Phys. Rev. Lett.* **97**, 228302 (2006).
16. Koshikiya, Y. & Hachisu, S. in *Proceedings of the Colloid Symposium of Japan* (in Japanese, 1982).
17. Pieranski, P., Strzelecki, L., & Pansu, B. Thin colloidal crystals. *Phys. Rev. Lett.* **50**, 900-903 (1983).
18. Van Winkle, D. H. & Murray, C. A. Experimental observation of two-stage melting in a classical two-dimensional screened. *Phys. Rev. A* **34**, 562-1203 (1986).
19. Weiss, J. A., Oxtoby, D. W., Grier, D.G. & Murray, C. A. Martensitic transition in a confined colloidal suspension. *J. Chem. Phys.* **103**, 1180-1190 (1995).
20. Pansu, B., Pieranski, Pi. & Pieranski, Pa. Direct observation of a buckling transition during the formation of thin colloidal crystals. *J. Physique* **45**, 331-339 (1984).
21. Chou, T. & Nelson, D. R. Buckling instabilities of a confined colloid crystal layer. *Phys. Rev. E* **48**, 4611-4621 (1993).
22. Schmidt, M. & Löwen, H. Freezing between two and three dimensions. *Phys. Rev. Lett.* **76**, 4552-4555 (1996).
23. Schmidt, M. & Löwen, H. Phase diagram of hard spheres confined between two parallel plates. *Phys. Rev. E* **55**, 7228-7241 (1997).
24. Zangi, R. & Rice, S. A. Phase transitions in a quasi-two-dimensional system. *Phys. Rev. E* **58**, 7529-7544 (1998).
25. P. Melby *et al.* The dynamics of thin vibrated granular layers. *J. Phys. Cond. Matt.* **17**, S2689-S2704 (2005).
26. Osterman, N., Babič, D., Poberaj, I., Dobnikar, J. & Zihnerl, P. Observation of condensed phases of quasipolar core-softened colloids. *Phys. Rev. Lett.* **99**, 248301 (2007).
27. Alsayed, A. M., Islam, M. F., Zhang, J., Collings, P. J. & Yodh, A. G. Premelting at defects within bulk colloidal crystals. *Science* **309**, 1207-1210 (2005).
28. Ogawa, T. A maze-like pattern in a monodisperse latex system and the frustration problem. *J. Phys. Soc. Jpn. Suppl.* **52**, 167-170 (1983).
29. Crocker, J. C. & Grier, D. G. Methods of digital video microscopy for colloidal studies. *J. Colloid Interface Sci.* **179**, 298-310 (1996).
30. Han, Y., Ha, N. Y., Alsayed, A. M. & Yodh, A. G. Melting of two-dimensional tunable-diameter colloidal crystals. *Phys. Rev. E* **77**, 041406 (2008).
31. Metcalf, B. D. Ground state spin orderings of the triangular Ising model with the nearest and next nearest neighbor interaction. *Phys. Lett. A* **46**, 325-326 (1974).
32. Millane, R. P. & Blakeley, N. D. Boundary conditions and variable ground state entropy for the antiferromagnetic Ising model on a triangular lattice. *Phys. Rev. E* **70**, 057101 (2004).
33. Chen, Z. Y. & Kardar, M. Elastic antiferromagnets on a triangular lattice. *J. Phys. C: Solid State Phys.* **19**, 6825-6831 (1986).
34. Gu, L., Chakraborty, B., Garrido, P. L., Phani, M. & Lebowitz, J. L. Monte Carlo study of a compressible Ising antiferromagnet on a triangular lattice. *Phys. Rev. B* **53**, 11985-11992 (1996).
35. Villain, J., Bidaux, R., Carton, J. P. & Conte, R. Order as an effect of disorder. *J. Physique* **41**, 1263-1272 (1980).
36. Mau, S. C. & Huse, D. A. Stacking entropy of hard-sphere crystals. *Phys. Rev. E* **59**, 4396-4401 (1999).
37. Liebmann, R. *Statistical Mechanics of Periodic Frustrated Ising Systems* (Springer-Verlag Berlin, Heidelberg, 1986).
38. Chakraborty, B., Gu, L. & Yin, H. Glassy dynamics in a frustrated spin system: the role of defects. *J. Phys. Condens. Matt.* **12**, 6487-6495 (2000).
39. Yin, H. & Chakraborty, B. Entropy-vanishing transition and glassy dynamics in frustrated spins. *Phys. Rev. Lett.* **86**, 2058-2061 (2001).
40. Nussinov, Z. Avoided phase transitions and glassy dynamics in geometrically frustrated systems and non-Abelian theories. *Phys. Rev. B* **69**, 014208 (2004).

**Acknowledgements** We thank Bulbul Chakraborty, Randy Kamien, Dongxu Li, Andrea Liu, Carl Modes, Tai-Kai Ng, Stuart Rice, Yehuda Snir, Tom Witten, and Yi Zhou for helpful discussions. This work is supported by NSF MRSEC grants DMR-0520020 and DMR-0505048.

**Author Information** Correspondence and requests for materials should be addressed to Y.S. (yair@sas.upenn.edu) or Y.H. (yilong@ust.hk).